RESEARCH ARTICLE

Structure and Dynamics of Large-Scale Cognitive Networks in Huntington's Disease

Ignacio Aracil-Bolaños, MD,[1,2,3,4] Saül Martínez-Horta, MSc,[1,2,3,4] Jose M. González-de-Echávarri, MD,[5] Frederic Sampedro, MD, PhD,[1,2,3,4] Jesús Pérez-Pérez, MD,[1,2,3,4] Andrea Horta-Barba, MSc,[1,2,3,4] Antonia Campolongo, BSc,[1,2,3,4] Cristina Izquierdo, BSc,[1,2,3,4] Beatriz Gómez-Ansón, MD, PhD,[2,3,4,6] Javier Pagonabarraga, MD, PhD,[1,2,3,4] and Jaime Kulisevsky, MD, PhD[1,2,3,4*]

[1]*Movement Disorders Unit, Neurology Department, Sant Pau Hospital, Barcelona, Spain*
[2]*Departament de Medicina, Universitat Autònoma de Barcelona, Barcelona, Spain*
[3]*Institut d'Investigacions Biomèdiques-Sant Pau, Barcelona, Spain*
[4]*Centro de Investigación en Red-Enfermedades Neurodegenerativas, Madrid, Spain*
[5]*Barcelonaβeta Brain Research Center, Pasqual Maragall Foundation and Hospital del Mar Medical Research Institute, Barcelona, Spain*
[6]*Neuroradiology Unit, Sant Pau Hospital, Barcelona, Spain*

ABSTRACT: Background: Huntington's disease is a neurodegenerative disorder characterized by clinical alterations in the motor, behavioral, and cognitive domains. However, the structure and disruptions to large-scale brain cognitive networks have not yet been established.
Objective: We aimed to profile changes in large-scale cognitive networks in premanifest and symptomatic patients with Huntington's disease.
Methods: We prospectively recruited premanifest and symptomatic Huntington's disease mutation carriers as well as healthy controls. Clinical and sociodemographic data were obtained from all participants, and resting-state functional connectivity data, using both time-averaged and dynamic functional connectivity, was acquired from whole-brain and cognitively oriented brain parcellations.
Results: A total of 64 gene mutation carriers and 23 healthy controls were included; 21 patients with Huntington's disease were classified as premanifest and 43 as symptomatic Huntington's disease. Compared with healthy controls, patients with Huntington's disease showed decreased network connectivity within the posterior hubs of the default-mode network and the medial prefrontal cortex, changes that correlated with cognitive ($t = 2.25$, $P = 0.01$) and disease burden scores ($t = -2.42$, $P = 0.009$). The salience network showed decreased functional connectivity between insular and supramarginal cortices and also correlated with cognitive ($t = 2.11$, $P = 0.02$) and disease burden scores ($t = -2.35$, $P = 0.01$). Dynamic analyses showed that network variability was decreased for default-central executive networks, a feature already present in premanifest mutation carriers (dynamic factor 8, $P = 0.02$).
Conclusions: Huntington's disease shows an early and widespread disruption of large-scale cognitive networks. Importantly, these changes are related to cognitive and disease burden scores, and novel dynamic functional analyses uncovered subtler network changes even in the premanifest stages. © 2021 The Authors. *Movement Disorders* published by Wiley Periodicals LLC on behalf of International Parkinson and Movement Disorder Society

Key Words: Huntington's; cognition; functional MRI

Huntington's disease (HD) is a neurodegenerative disorder caused by an abnormal CAG repeat expansion in the *HTT* gene on chromosome 4.[1] The clinical onset of the disease is marked by the presence of unequivocal extrapyramidal movement disorders—such as chorea, dystonia, or bradykinesia—but cognitive and

*Correspondence to: Dr. J. Kulisevsky, Movement Disorders Unit, Neurology Department, Sant Pau Hospital, Mas Casanovas 90-08041, Barcelona, Spain; E-mail: jkulisevsky@santpau.cat

Relevant conflicts of interest/financial disclosures: Nothing to report.

Funding agencies: This study was supported by the Fondo de Invetigaciones Sanitarias of the Spanish government (J.P.P.; Grant PI17/001885) and the Huntington's Disease Society of America (S.M.-H.; grant title "HD Human Biology Project").

[Correction added on 20 January 2022, after first online publication: The name of author Andrea Horta has been updated to Andrea Horta-Barba.]

Received: 8 June 2021; **Revised:** 10 September 2021; **Accepted:** 4 October 2021

Published online in Wiley Online Library (wileyonlinelibrary.com). DOI: 10.1002/mds.28839

behavioral features can be detected up to 15 years before the emergence of the first motor symptoms.[2] Subtle cognitive changes are present from the early stages, with the development of dementia as a likely outcome in the majority of the cases.[3] The progression of cognitive decline has been attributed to a pattern of whole-brain atrophy, with the basal ganglia and its fronto-subcortical connections as the most affected by disease progression.[4] However, recent works have shown that progressive atrophy of a wide range of cortical regions is linked to the clinical profile of the disease from the early stages. This cortical atrophy involves several regions that participate in cognitive functions such as the precuneus,[5] the anterior cingulate cortex,[6] and the supramarginal, fusiform, and lateral occipital gyrii.[7] The majority of these regions are integral to the functioning of large-scale cognitive networks,[8] such the salience network (SN) or default-mode network (DMN). Thus, cognitive manifestations of HD might be related both to structural brain damage and the disruptions in the architecture of large-scale brain cognitive networks.

Structural damage in the basal ganglia and motor and visual regions has been shown to correlate with alterations in both motor and visual functional networks,[9,10] even from the premanifest stage.[11,12] Studies focusing on the DMN using resting-state functional magnetic resonance imaging (fMRI) showed decreases in functional connectivity (FC) within the network in manifest HD but no changes in premanifest patients.[13] In this latter population, task-based fMRI found an increased connectivity within the DMN.[14] In the executive networks, a dissociated pattern was found between posterior cortical decreases in activity[10] and an increase in frontoparietal connectivity,[15] but again, studies in the premanifest population have shown no differences.[16]

Finally, to our knowledge, no study has tackled the study of dynamic FC of cognitive networks in HD. Although static FC has proven to be demonstrable across task and resting-state conditions,[17] and even across species,[18] there is growing evidence that brain networks are not immutable across time, but inherently "multistable."[19] This includes the notion that cognitive hubs such as the posterior cingulate cortex (PCC) can dynamically engage with different networks.[20,21] Previous studies have established the relevance of the frequency of connectivity states in the cognition of neurodegenerative diseases such as Parkinson's disease,[22] showing that patients with an associated dementia have a higher frequency of a segregated connectivity state than healthy controls. On the other hand, high variability of these connectivity circuits is considered to be a feature of normal organization in the brain[23] that decreases with normal aging[24]; it has also been found to be decreased within default-mode and frontoparietal networks in patients with schizophrenia.[25] It is conceivable that the subtler aspects of network disruption could become more apparent when considering the dynamic nature of brain circuits.

The main aim of the present study was to conduct a functional analysis of the different large-scale cognitive networks in premanifest HD (pre-HD) and symptomatic HD (sHD). Although cognitive manifestations may represent the earliest indicators of the disease, there is a lack of studies exploring the integrity of cognitive networks and its clinical impact on HD. Specifically, we performed classical averaged FC and graph theory analyses, and we also conducted a novel dynamic FC analysis through dynamic independent component analysis (dyn-ICA). We also performed a structural analysis of brain atrophy using cortical thickness while adopting both a standard whole-brain approach and a cognitive network-focused parcellation, similar to our previous work.[26]

Patients and Methods

Participants and Clinical Assessment

A total of 65 gene mutation carriers (CAG ≥ 39) who attended the outpatient clinic at the Movement Disorders Unit and 23 healthy controls who were willing to participate were prospectively recruited. Patients with HD were classified as premanifest HD (pre-HD) and sHD. Individuals with a Unified Huntington's Disease Rating Scale (UHDRS) total motor score below 5 and a diagnostic confidence level (DCL) <3 were classified as pre-HD, whereas those with a DCL = 4 were classified as sHD. Cognitive measures were obtained using the UHDRS cognitive score (Cogscore). The disease burden score (DBS)—a measure of livelong exposure to mutant huntingtin—was calculated using the following formula based on age and CAG repeat length: age × (CAG − 35.5).[27] However, healthy controls only had sociodemographic data available. Exclusion criteria based on image quality were (1) pathological magnetic resonance imaging (MRI) findings beyond mild white matter hyperintensities and (2) the presence of head motion or other MRI artifacts. After reviewing images for quality control, one patient was excluded because of excessive head motion.

MRI Acquisition and Preprocessing

All participants had available structural and resting-state fMRI. Details regarding image acquisition and preprocessing are available in Appendix S1 in the supplementary material. Briefly, T1-weighted scans and resting-state (blood-oxygen-level-dependent) BOLD images (12 minutes) were acquired in a 3 T Philips Achieva station (Philips Medical System, Best, the Netherlands). To assess cortical atrophy differences we

applied a surface-based cortical thickness pipeline using FreeSurfer 6.0. (free software: Fisch et al, 10.1016/j.neuroimage.2012.01.021) Functional imaging processing was performed using CONN v19b software and its standard processing pipeline,[28] which includes functional preprocessing and brain parcellation and first-level and second-level analyses steps. For preprocessing, scans were functionally realigned and unwarped, slice-timing corrected, realigned, and spatially normalized to the Montreal Neurological Institute (MNI) space using coregistration with the associated anatomical data. For brain parcellation, we adopted both the Harvard-Oxford Atlas[29] provided within the CONN toolbox and the set of functional brain networks described in the Shirer atlas[30] to provide both whole-brain macroanatomical coverage and functionally oriented parcellations[31]; time courses for all of these regions of interest (ROIs) were derived from MNI-normalized images. Thereafter, ROI time courses were submitted to CONN's standard denoising pipeline, which combines linear regression of potential confounding effects and temporal band-pass filtering. For the first-level signal processing, we adopted both time-averaged static FC measures and a dyn-ICA. Dyn-ICA matrices represent a measure of different modulatory circuits expression and rate of connectivity change between each pair of ROIs. For the second-level analysis, averaged metrics of FC and graph theoretical parameters were computed in ROI-to-ROI analyses as well as dyn-ICA parameters: frequency was defined as the recurrence of the modulatory circuits in each participant and variability as the standard deviation in bivariate, multivariate, or semipartial correlation or regression measures between pairs of ROIs. A detailed description of the preprocessing, denoising, and first-level and second-level analyses as well as an in-depth discussion of dyn-ICA parameters is provided in Appendix S1 in the supplementary material.

Statistical Analyses

Clinical and sociodemographic data were compared across groups using two-sample t test analyses for continuous variables and χ^2 for categorical variables. Differences were considered significant using a probability (P) value < 0.05. On the structural analyses, only surface clusters surviving $P < 0.05$ family-wise error corrected by permutation were considered.

On the structural analysis, we compared vertex-wise cortical thickness data between HD (pre-HD/sHD) and healthy controls using age, sex, and education as nuisance covariates. For this purpose, vertex-wise cortical thickness maps were normalized to a standard fsaverage space and smoothed using a Gaussian kernel of 10 mm full width at half maximum. Only surface clusters surviving $P < 0.05$ and family-wise error correction by permutation testing (10,000 permutations) were considered significant.

Functional and graph theoretical metrics were introduced into a generalized linear model within CONN to compare controls, pre-HD groups, and sHD groups using age, sex, and education as covariates of no interest. Furthermore, total gray matter volume was explored as a covariate of no interest to analyze the interaction between functional and structural changes. Results were considered significant using a threshold of P value < 0.05 corrected for multiple comparisons at the cluster level using the false discovery rate for all the functional and graph theoretical analyses. Temporal data regarding dyn-ICA analysis of frequency and variability of dynamic components were also introduced into

TABLE 1 *Demographics, genetics, and clinical data of the study population, according to disease stage*

Variables	HD	Pre-HD	Symptomatic HD	Healthy controls	HD vs. controls, *P* value	Pre-HD vs. symptomatic HD, *P* value
N	64	21	43	23		
Age, y	45.77 ± 12	38.33 ± 7.5	49.4 ± 12.1	39.34 ± 9.3	0.01	<0.001
Sex	41/64 women	15/21 women	26/43 women	8/23	0.92	0.76
Education, y	13 ± 4.1	14.05 ± 3.3	12.08 ± 4.36	12 ± 1.6	0.05	0.03
CAG repeats	43.18 ± 2.6	42.7 ± 2.2	43.4 ± 2.85	N/A	N/A	0.88
UHDRS	17.55 ± 20	0.3 ± 0.7	25.95 ± 19.6	N/A	N/A	<0.001
Cogscore	240.39 ± 97	328.33 ± 46.7	195.34 ± 85	N/A	N/A	<0.001
Disease burden score	334.49 ± 108	266.53 ± 77.5	367.64 ± 105.3	N/A	N/A	<0.001
Years to disease onset	N/A	14.5 ± 6.07	N/A	N/A	N/A	

Data are provided as n or mean ± standard deviation.
Abbreviations: HD, Huntington's disease; N/A, Not available; UHDRS, Unified Huntington's Disease Rating Scale.

a generalized linear model using age, sex, and education as covariates of no interest and considered significant using a P value < 0.05. Finally, regression analyses were performed using DBS, UHDRS, and Cogscore data in the relevant connections (which had previously been found as statistically significant between groups in a $P < 0.05$ corrected analysis) and dynamic components and considered significant using a P value of <0.05. Statistical analyses concerning clinical and sociodemographic comparisons as well as clinical imaging associations were conducted using the SPSS version 15 (IBM Corp. Armonk, NY) software package.

All patients provided written informed consent according to the Declaration of Helsinki. The study was approved by the Ethics Comitee for Clinical Research at the Hospital de la Santa Creu i Sant Pau.

Results

Clinical and Sociodemographic Data

A total of 64 gene mutation carriers (mean age, 45.77 ± 12 years; mean CAG, 43.18 ± 2.6; mean DBS, 334.49 ± 108) and 23 healthy controls (mean age, 39.34 ± 9.3 years) were included; 21 patients with HD were classified as pre-HD (mean age, 38.3 ± 7.5 years; mean CAG, 42.7 ± 2.2; mean DBS, 266.53 ± 57.5) and 43 were classified as sHD (mean age, 49.4 ± 12 years;

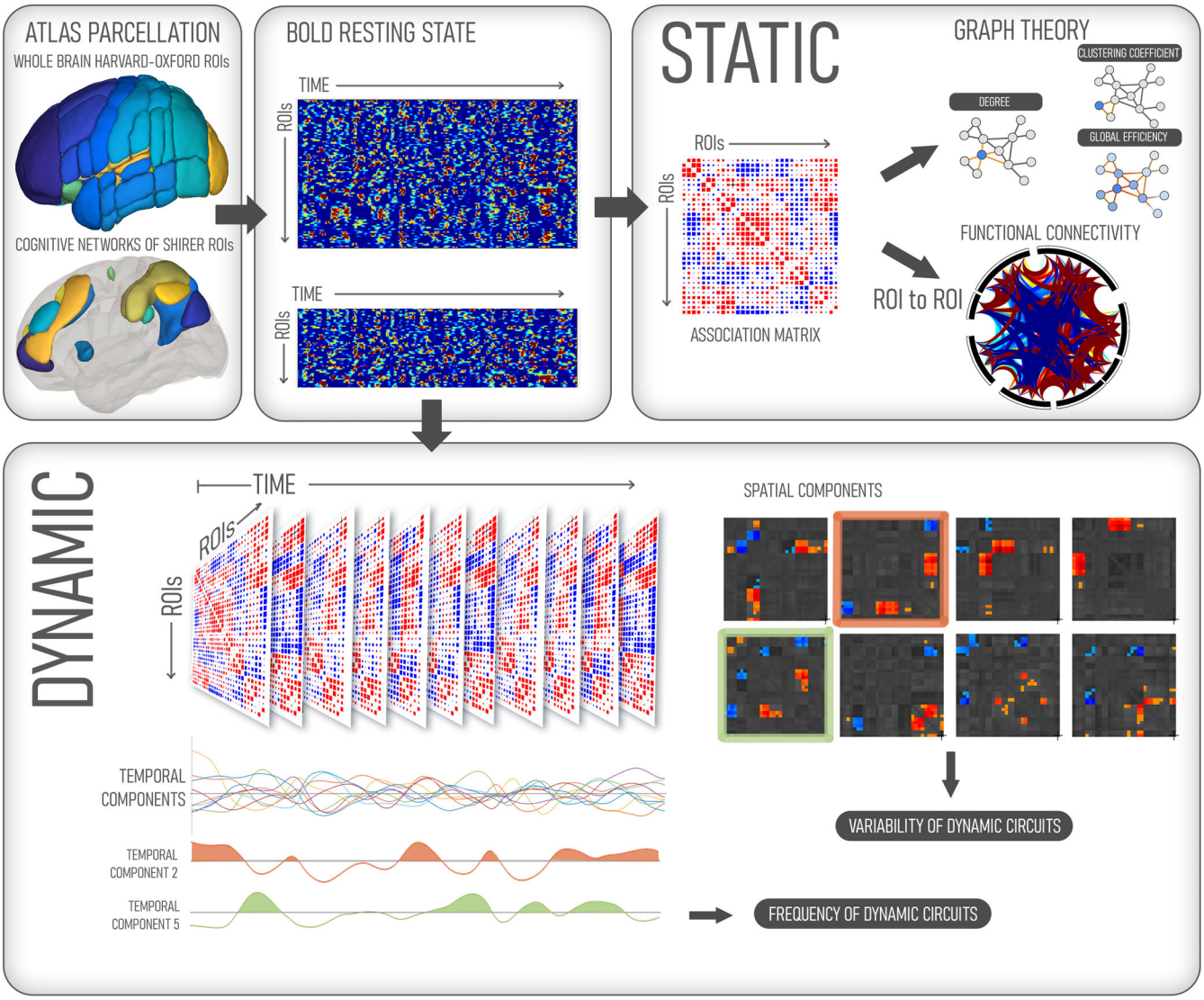

FIG. 1. Summary of the imaging analysis methodology. On the upper left corner, the two parcellations (whole-brain Harvard-Oxford and the cognitive networks of the Shirer atlas) are used to obtain the time series of their respective brain regions. These time series are averaged to produce static association matrices that result in region-of-interest (ROI) functional connectivity data and network architectural analysis via graph theory. On the lower half of the picture, time series are analyzed using a dynamic independent component analysis (dyn-ICA), which identifies changes in temporal fluctuations of the dynamic components (frequency) and in spatial relations between the components (variability). [Color figure can be viewed at wileyonlinelibrary.com]

mean CAG, 43.4 ± 2.85; mean DBS, 367.64 ± 105.3). For full demographic data, see Table 1.

Patients with pre-HD were comparable in age and sex to controls but had a slightly higher education level (14 vs. 12 years for controls). Patients with sHD were older than controls (49 vs. 39 years in controls). All of these differences were accounted for in imaging analyses by using these variables as covariates of no interest.

Structural Analysis: Cortical Thickness

On the structural analysis, patients with HD showed reduced widespread cortical thinning in frontal, parietal, and temporo-occipital regions. These changes were more pronounced when comparing patients with sHD with healthy controls, whereas patients with pre-HD showed no differences in cortical thickness relative to controls. Figure 1 and Appendix S1 in the supplementary material display the cortical thickness differences between these groups.

Time-Averaged FC

Whole-Brain FC

On a whole-brain approach, patients with HD showed decreased FC on a wide range of cortical regions, chiefly the motor cortex (Fig. 2, left). Precentral, postcentral, and supplementary motor areas showed decreased FC with visual associative cortices ($P = 0.002$ corrected) and fronto-opercular regions, including the bilateral insular and anterior cingulate cortices ($P = 0.01$ corrected). Importantly, these decreases were clinically associated with both the UHDRS scores and with the DBS. The regression analysis showed that reduced FC between the postcentral gyrus and the occipital fusiform gyrus was associated with higher DBS ($t = -2.57$, $P = 0.006$) and UHDRS ($t = -5.27$, $P < 0.001$), and similarly, decreased FC between the right insular and supplementary motor cortex was correlated with higher DBS ($t = -2.83$, $P = 0.003$) and UHDRS ($t = -4.73$, $P < 0.001$). The basal ganglia also showed reduced connections with the superior and mid frontal gyrii ($P = 0.01$ corrected).

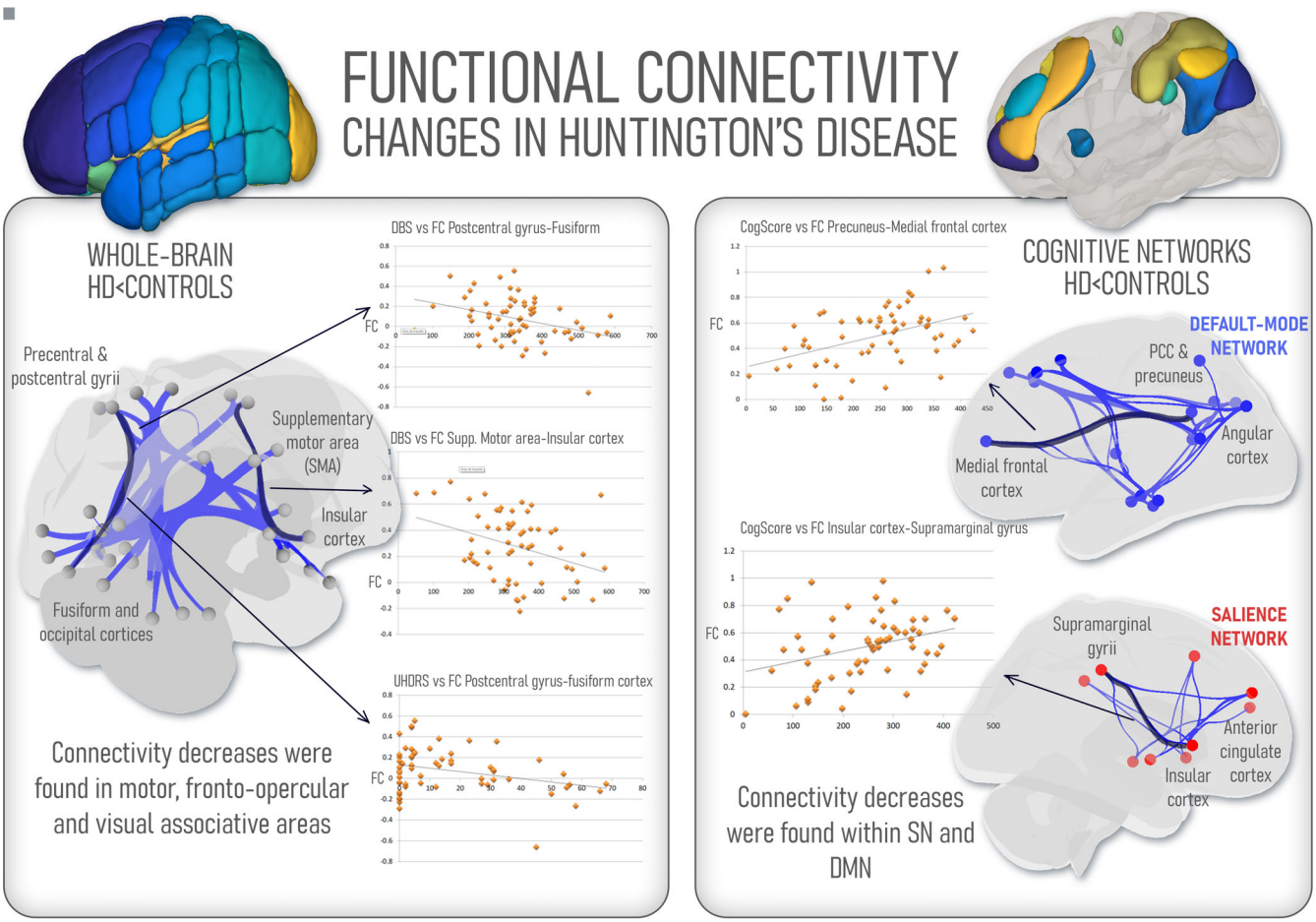

FIG. 2. Changes in region-of-interest (ROI)-to-ROI functional connectivity between patients with Huntington's disease (HD) and healthy controls both using a global brain parcellation (left) and a cognitive networks parcellation (right). DMN, default-mode network; PCC, posterior cingulate cortex; SN, salience network. [Color figure can be viewed at wileyonlinelibrary.com]

Specifically, reduced caudate–mid frontal gyrus connections were associated with higher DBS ($t = -2.98$, $P = 0.002$) and UHDRS ($t = -2.60$, $P = 0.004$) for the caudate–mid frontal gyrus connections. The main increase in FC among patients with HD compared with controls was found between visual regions—fusiform cortex, occipital pole—and the PCC and precuneus, both cortical hubs of the DMN ($P = 0.003$ corrected). The regression analysis showed that higher FC between the precuneus and the right fusiform cortex was associated with higher DBS ($t = 1.99$, $P = 0.02$).

FC in Cognitive Networks

Considering cognitive networks, patients with HD showed decreased connectivity within posterior hubs of the DMN such as the precuneus and PCC, and of these hubs with anterior regions of the same network such as the medial prefrontal cortex ($P < 0.001$ corrected; Fig. 2, right). A key aspect is that the posterior cingulate cortex (PCC)-Med frontal connection showed a positive correlation with cognitive scores as measured by the Cogscore ($t = 2.25$, $P = 0.01$) and an inverse correlation with DBS ($t = -2.42$, $P = 0.009$). The salience network of patients with HD showed decreased FC between insular, supramarginal, and anterior cingulate cortices ($P = 0.009$), and the connection between the right insular and supramarginal regions also showed a positive correlation with the Cogscore ($t = 2.11$, $P = 0.02$) and an inverse correlation to DBS ($t = -2.35$, $P = 0.01$).

FC in Pre-HD

Patients with pre-HD showed similar results both on a whole-brain and cognitive networks approach, albeit in a reduced fashion. Differences with healthy controls were centered on motor and visual associative regions on a whole-brain approach ($P = 0.02$ corrected), and connectivity increases between the PCC/precuneus and visual associative regions were also observed ($P = 0.04$ corrected). Meanwhile, in cognitive networks, changes were mainly observed as decreases of connectivity between anterior and posterior nodes of the DMN ($P = 0.02$).

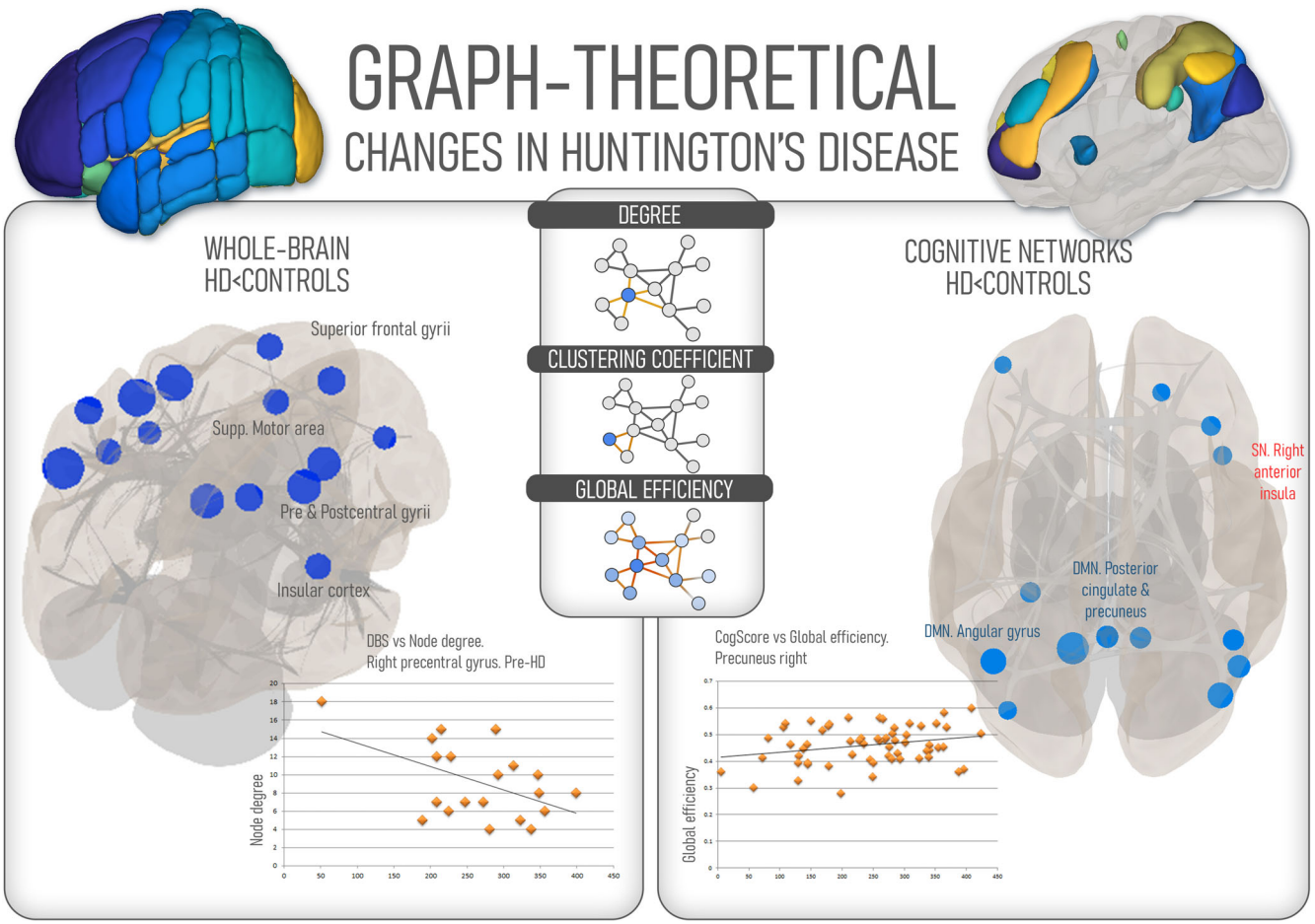

FIG. 3. Graph theoretical changes in Huntington's disease (HD) compared with healthy controls, according to both global and cognitive-oriented parcellations. Regressions with clinical parameters (disease burden score and Cogscore) are shown in the lower part of the image. DBS, disease burden score; DMN, default-mode network; PCC, posterior cingulate cortex; SN, salience network [Color figure can be viewed at wileyonlinelibrary.com]

Importantly, after controlling for gray matter volume (GMV), all results remained significant with the following exceptions: in patients with pre-HD, increased precuneus/PCC connectivity with visual associative regions in a whole-brain approach (not present after correcting for GMV) and decreases in connectivity between anterior and posterior nodes of the DMN ($P = 0.06$ after correcting for GMV).

Graph Theoretical Metrics

Whole-Brain Graph Metrics

On a whole-brain analysis, patients with HD showed decreased node degrees compared with controls in bilateral postcentral and precentral gyrii ($P = 0.007$ corrected) and the supplementary motor area ($P = 0.04$ corrected) and decreases in other nonmotor regions such as the bilateral supramarginal gyrus ($P = 0.04$ corrected) and the PCC ($P = 0.006$ corrected; Fig. 3, left). All of these regions also showed a reduction in global efficiency, and in the left postcentral gyrus, decreases in node degree and global efficiency were correlated with higher UHDRS scores in patients with manifest HD ($t = -2.31$, $P = 0.01$), whereas a lower node degree was correlated with higher DBS in pre-HD ($t = -1.98$, $P = 0.03$).

Graph Metrics in Cognitive Networks

Using a cognitive networks approach, decreases in node degree were found on the bilateral precuneus ($P = 0.02$ corrected), bilateral angular ($P = 0.02$ corrected), occipital ($P = 0.03$ corrected), and parahipoccampal gyrii ($P = 0.03$ corrected)—all DMN nodes—and the right anterior insula from the SN ($P = 0.04$ corrected; Fig. 3, right). Clustering coefficient was also reduced in the PCC ($P = 0.001$ corrected) and left anterior insula ($P = 0.02$ corrected). Finally, global efficiency was decreased in the right precuneus ($P = 0.03$ corrected). This decrease correlated directly with the Cogscore ($t = 2.23$, $P = 0.01$).

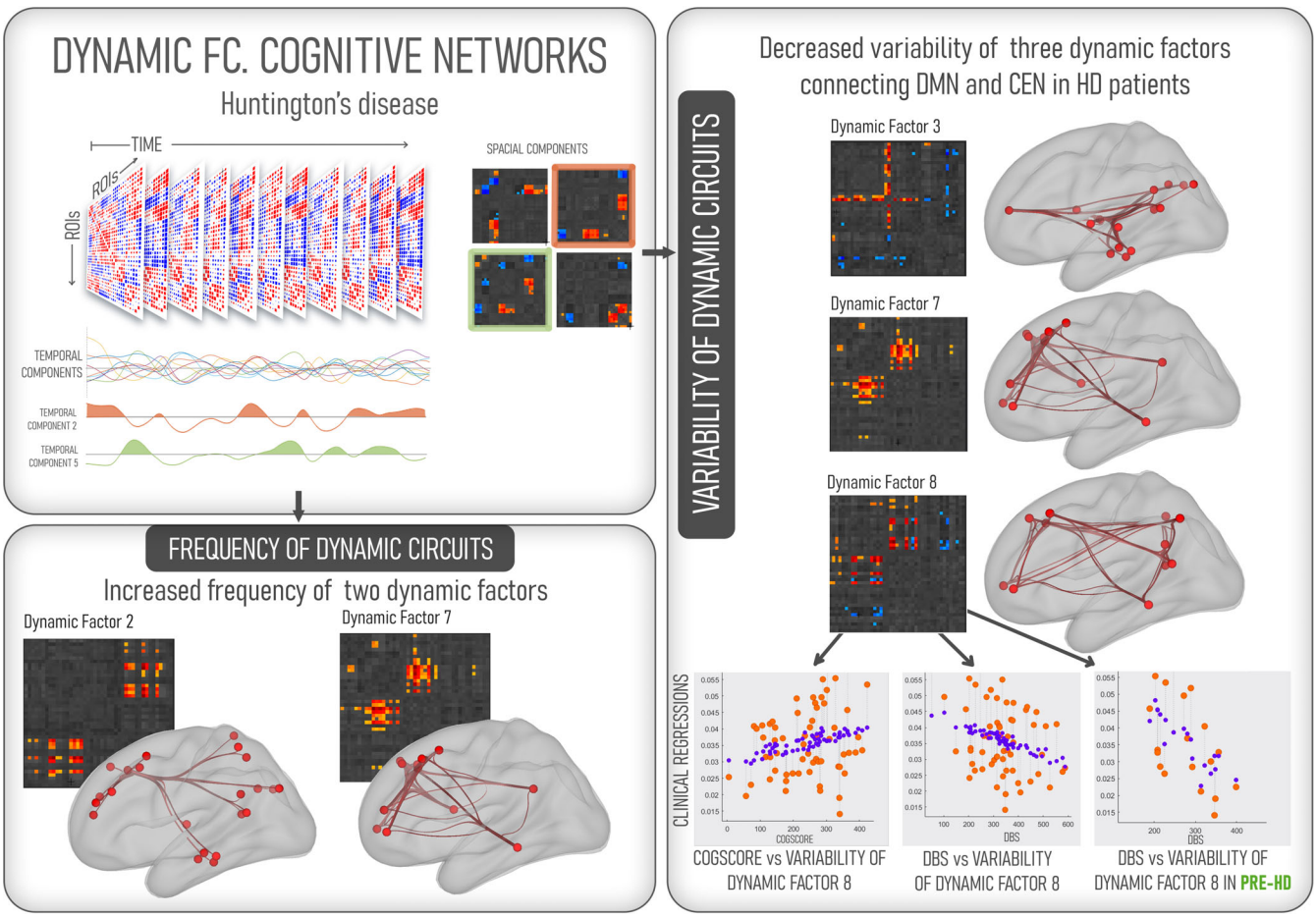

FIG. 4. Analysis of dynamic factors in patients with Huntington's disease (HD) compared with healthy controls. On the lower left, dynamic factors that showed increased frequency in patients with HD are shown. On the right, decreases in variability of three dynamic factors compared with healthy controls; on the lower part, clinical regressions are shown related to the loss of variability in dynamic factor 8. DMN, default-mode network; ROI, region of interest; CEN, Central executive network. [Color figure can be viewed at wileyonlinelibrary.com]

Graph Metrics in Pre-HD

On a whole-brain approach, the pre-HD group showed similar decreases in node degree compared with controls, centered around bilateral precentral and postcentral gyrii and the PCC (all $P = 0.03$ corrected). We also found that some of these nodes—the bilateral precentral and postcentral gyri—also showed decreased global efficiency compared to controls. Furthermore, path length was increased in motor and nonmotor regions of the cortex, including the bilateral insular cortex, bilateral fusiform gyri, and the bilateral amygdalae (all $P = 0.04$ corrected). Considering cognitive networks, pre-HD already showed a loss of clustering coefficient in the PCC ($P = 0.01$ corrected) and the left anterior insula ($P = 0.03$ corrected).

After controlling for GMV, all results remained significant with the following exceptions: node degree decreases in the supplementary motor area ($P = 0.06$ corrected after controlling for GMV); clustering coefficient decreases in the left anterior insula ($P = 0.09$ corrected after controlling for GMV); global efficiency decreases in the left precuneus ($P = 0.06$ corrected after controlling for GMV); and in pre-HD, path length increases in bilateral insular cortex and bilateral amygdalae (not present after controlling for GMV) and clustering coefficient decreases in the PCC and left anterior insula (not present after correcting for GMV).

Dynamic Independent Component Analysis

A total of 12 dynamic factors corresponding to within-network and between-network connectivity patterns were identified in the whole sample: 4 components captured SN-DMN interactions, 4 identified CEN-DMN interactions, 1 corresponded to CEN-SN interactions, and 3 corresponded to within network connections. The outlook of the 12 dynamic factors is displayed in Appendix S1 in the supplementary material and Figure 2.

Comparing the HD group with healthy controls, patients had higher frequencies of DMN-CEN coupling, with the strongest connections between parahippocampal and precuneus DMN and orbitofrontal Central executive network (CEN) (factor 7, $P = 0.04$), whereas the controls showed an increased frequency of dynamic SN-DMN connections, highlighted by the links between the anterior cingulate and frontal cortex with the bilateral precuneus of the DMN (factor 2, $P = 0.03$; Fig. 4, bottom left). On the variability analysis, all of the dynamic factors showed increases in controls, related to DMN-CEN couplings, in which the right caudate of the CEN shows increased dynamic connectivity with DMN structures such as the bilateral precuneus, bilateral angular, and bilateral occipital cortices (factor 7, $P = 0.04$; factor 3, $P = 0.03$; factor 8, $P = 0.002$; Fig. 4, right). After performing a post hoc correction for the number of dynamic factors, only the variability of factor 8 remained statistically significant ($P < 0.05$ corrected). Importantly, the variability of factor 8, which connects frontal nodes of the CEN and posterior hubs of the DMN such as the PCC and precuneus, was directly correlated to the Cogscore ($t = 1.98$, $P = 0.02$) and inversely with the DBS ($t = -2.32$, $P = 0.02$).

Comparing pre-HD with controls, the controls preserve the higher frequency in the previously mentioned SN-DMN component (factor 2, $P = 0.04$), and variability remained higher for the DMN-CEN coupling in the control group, with higher connectivity between the frontal CEN hubs and the bilateral precuneus (factor 8, $P = 0.02$). The variability of factor 8 also correlated inversely with DBS in patients with pre-HD ($t = -2.60$, $P = 0.02$). Comparing pre-HD with sHD, the latter group presented a higher frequency of within-SN connections, highlighted by insular–precuneus connections (factor 4, $P = 0.04$), whereas patients with pre-HD showed an increased variability in SN connectivity, mainly insular cortex, with frontal regions of both the DMN and CEN (factor 9, $P = 0.04$).

Discussion

In the present study, we analyzed the landscape of FC changes associated with pre-HD and manifest HD and how they compare to healthy controls. Adopting both a whole-brain and a cognitive networks approach, we found commonalities with previous descriptions of brain networks in HD, but also a number of salient points that are derived from newer approaches such as dynamic FC analysis. We also examined the brain atrophy of the patients with HD compared with healthy controls to frame this functional analysis.

In patients with HD, widespread cortical thinning was observed compared with healthy controls. This pattern of extensive atrophy has been previously reported by our group[7,32] and others[2,4] and shows that the loss of cortical thickness occurs in frontal, temporo-parietal, and occipital cortices in patients with HD. Patients with pre-HD showed no differences compared with healthy controls using stringent statistical thresholds, a fact that has been shown in previous studies in patients with early HD,[33] although others have shown cortical thinning in the early stages.[5] However, this could be explained by the long time to onset in the patients with pre-HD in our sample (14.05 ± 6 years; see Table 1) because previous studies have shown almost no cortical thinning in patients with an estimated onset to disease higher than 5 years.[2] Furthermore, we observed that the structural changes did not have a pronounced effect in the functional analyses when gray matter volume was used as a covariate of no interest.

Using a whole-brain parcellation scheme, the changes in FC observed in our sample were mainly related to visual associative and motor regions. These changes

involved the fusiform gyrus, occipital pole, and precentral/postcentral cortices and were also found when comparing patients with pre-HD with healthy controls. In previous studies, reduced FC in the somatomotor cortex has been related to the severity of motor symptoms.[9,10] Similarly, the visual networks have shown reduced FC in HD,[12] and this decrease was related to impairment in visual scanning and motor speed. Therefore, the reduced FC between motor and visual associative regions in our sample could underlie these clinical changes that are present, albeit in a reduced fashion, even in the premotor stage.[34] Importantly, these changes in our sample were linked to increasing disease burdens and worse motor scores. Graph theoretical findings also support these results, showing decreased degree and efficiency in precentral and postcentral hubs even in the premotor stage, and a widespread increase in path lengths across the network, signaling a decrease in the efficient transfer on information across its nodes. Of note, some cognitive regions were highlighted in this global analysis, mainly via an increase of FC between the PCC and the visual associative cortex, which correlates with higher DBSs. However, these changes are much less prominent compared with the visuomotor impairment.

The cognitive networks approach showed that patients with HD lose connectivity in the major large-scale networks in the resting state. These decreases were particularly consistent regarding the DMN, which had already been reported in sHD.[10,13,35] In our sample, decreases of FC affected key nodes of the DMN, and this reduced connectivity translated into lower Cogscores as well as higher DBSs, especially for connections between the anterior and posterior components of the DMN. Furthermore, these decreases were accompanied by lower node degree, clustering coefficients, and global efficiency properties in these nodes, the latter showing a correlation with cognitive scores. Changes outside of FC had previously been documented only in relation with depression[36] or using regional metrics such as amplitude of low-frequency fluctuations.[37] More significant for us were the decreases found within the SN, which had not been found in previous studies of cognitive networks in HD.[38] We found a loss of FC within SN hubs such as the insula, the supramarginal gyrus, and the anterior cingulate and a further decrease in node degree and efficiency in the anterior insula. These changes were again correlated with clinical outcomes both in cognitive and DBSs. These findings are important given that the SN plays a critical role in the attribution and signaling of relevant inner and external information and thus in the engagement of goal-directed behavior and emotional processing.[39] Therefore, our findings may provide new insights on the functional mechanisms leading to the reduction on goal-directed behavior and emotional processing observed in HD.[34] We also found disruptions in these networks in the premanifest group, with lower FC within the DMN and decreased clustering coefficients both in the SN and DMN.

All of these concepts, however, are based on the premise that FC is "static" across resting-state acquisition, a concept that seems at odds with the dynamic nature of brain functioning. Reconciling classical resting-state network knowledge with a dynamic approach is challenging, but canonical large-scale networks could be considered as approximate static representations of the underlying dynamic brain.[40] Using dyn-ICA, we tried to retain the spatial identification of classical cognitive networks while adding temporal data such as frequency and variability, and we obtained two main conclusions. First, our results show that the dynamic connection between SN and DMN is less frequent in HD. These two networks were the most affected by the loss of intrinsic connectivity and topographical features in time-averaged analyses, and our results show that their interplay is also disrupted in a dynamic framework. An altered relationship between the SN and DMN can be found in previous static analyses of neurodegenerative diseases as a loss of anticorrelations,[26,41,42] but so far, to our knowledge, not in a dynamic framework. Our results lead us to believe that a time-dependent connection between these supposedly anticorrelated networks might be a trait of healthy participants and become lost in HD. This effect might probably be related to the SN's role as a "network fulcrum"—pivoting between executive and default-mode predominant settings—a concept proposed since the independent description of this network[43] that has been further confirmed using dynamic causal modeling.[44] Second—and perhaps more important given its clinical repercussion—although patients with HD show a higher frequency of DMN-CEN connections, their variability seems to be decreased across different dynamic factors. Above all, this loss in the dynamic interplay of the CEN and the DMN correlates with worse cognitive scores and higher DBS and can be found even in the premanifest group. Variability in brain networks is related to cognitive performance[45] and decreases with age,[24] and it could be conceived of as the repertoire of possible configurations of a brain network.[23] Thus, patients with HD seem to have a decreased range of network configurations that link DMN hubs, such as the precuneus, with CEN hubs such as the caudate nucleus. This altered dynamic resulted in worse clinical outcomes and is related to a more severe disease in our sample. We speculate that this lack of variability might be compensated by a higher frequency of this state, suggesting that CEN-DMN connections may assume maladaptive configurations that trade reduced efficiency for higher coupling.

We acknowledge some limitations to this study. First, cognition was explored mainly via the Cogscore, a

widely employed and validated tool for cognitive assessment in HD. However, detailed neuropsychological evaluation might reveal more subtle disruptions of cognitive function, especially in patients with pre-HD, in which we found fewer cognitive correlations with networks disruption. Further studies will need to evaluate the link between more precise clinical evaluation and network dysfunction. Second, our resting-state acquisition time might not sufficiently represent all the dynamic variability of the HD brain; however, given the intrinsic difficulties of imaging acquisition in patients (especially given the disease-specific symptoms such as chorea) we believe this is a realistic rendering of the dynamic brain states in these patients. Third, healthy controls only had sociodemographic data available in this study. Finally, the choice of cortical parcellation could influence the results, and it is still up for debate as recent publications show.[46] However, we think this work strikes a balance between whole-brain, microanatomical, and functionally oriented parcellations as has been suggested in recent reviews.[31]

Conclusions

To sum up, our results show that cognitive networks in HD are particularly affected, even in the premotor stages of the disease. These disruptions follow well-known patterns in neurodegenerative disease, with decreases in the intrinsic connectivity of the networks and the loss of graph-theoretical properties. Furthermore, a dynamic approach uncovers network interactions unapparent in static analyses of FC that extend into the premanifest stage. Further studies will be needed to replicate these findings and link them to the diverse phenotypical and neuropsychological aspects of HD. ●

DATA AVAILABILITY STATEMENT

The data that support the findings of this study are available from the corresponding author upon reasonable request

References

1. Ross CA, Aylward EH, Wild EJ, et al. Huntington disease: natural history, biomarkers and prospects for therapeutics. Nat Rev Neurol 2014;10(4):204–216. https://doi.org/10.1038/nrneurol.2014.24.
2. Tabrizi SJ, Langbehn DR, Leavitt BR, et al. Biological and clinical manifestations of Huntington's disease in the longitudinal TRACK-HD study: cross-sectional analysis of baseline data. Lancet Neurol 2009;8(9):791–801. https://doi.org/10.1016/S1474-4422(09)70170-X.
3. Peavy GM, Jacobson MW, Goldstein JL, et al. Cognitive and functional decline in Huntington's disease: dementia criteria revisited. Mov Disord 2010;25(9):1163–1169. https://doi.org/10.1002/mds.22953.
4. Dogan I, Eickhoff SB, Schulz JB, et al. Consistent neurodegeneration and its association with clinical progression in Huntington's disease: a coordinate-based meta-analysis. Neurodegener Dis 2013;12(1):23–35. https://doi.org/10.1159/000339528.
5. Rosas HD, Hevelone ND, Zaleta AK, Greve DN, Salat DH, Fischl B. Regional cortical thinning in preclinical Huntington disease and its relationship to cognition. Neurology 2005;65(5):745–747. https://doi.org/10.1212/01.wnl.0000174432.87383.87.
6. Nopoulos PC, Aylward EH, Ross CA, et al. Cerebral cortex structure in prodromal Huntington disease. Neurobiol Dis 2010;40(3):544–554. https://doi.org/10.1016/j.nbd.2010.07.014.
7. Martinez-horta S, Sampedro F, Horta-barba A, et al. Structural brain correlates of dementia in Huntington's disease. Neuroimage Clin 2020;28:102415. https://doi.org/10.1016/j.nicl.2020.102415.
8. Menon V. Large-scale brain networks and psychopathology: a unifying triple network model. Trends Cogn Sci 2011;15(10):483–506. https://doi.org/10.1016/j.tics.2011.08.003.
9. Müller HP, Gorges M, Grön G, et al. Motor network structure and function are associated with motor performance in Huntington's disease. J Neurol 2016;263(3):539–549. https://doi.org/10.1007/s00415-015-8014-y.
10. Poudel GR, Egan GF, Churchyard A, Chua P, Stout JC, Georgiou-Karistianis N. Abnormal synchrony of resting state networks in premanifest and symptomatic Huntington disease: the IMAGE-HD study. J Psychiatry Neurosci 2014;39(2):87–96. https://doi.org/10.1503/jpn.120226.
11. Coppen EM, van der Grond J, Hafkemeijer A, Barkey Wolf JJH, Roos RAC. Structural and functional changes of the visual cortex in early Huntington's disease. Hum Brain Mapp 2018;39(12):4776–4786. https://doi.org/10.1002/hbm.24322.
12. Wolf RC, Sambataro F, Vasic N, et al. Abnormal resting-state connectivity of motor and cognitive networks in early manifest Huntington's disease. Psychol Med 2014;44(15):3341–3356. https://doi.org/10.1017/S0033291714000579.
13. Quarantelli M, Salvatore E, Delle Acque Giorgio SM, et al. Default-mode network changes in Huntington's disease: an integrated MRI study of functional connectivity and morphometry. PLoS One 2013;8(8):e72159. https://doi.org/10.1371/journal.pone.0072159.
14. Wolf RC, Sambataro F, Vasic N, et al. Default-mode network changes in preclinical Huntington's disease. Exp Neurol 2012;237(1):191–198. https://doi.org/10.1016/j.expneurol.2012.06.014.
15. Werner CJ, Dogan I, Saß C, et al. Altered resting-state connectivity in Huntington's disease. Hum Brain Mapp 2014;35(6):2582–2593. https://doi.org/10.1002/hbm.22351.
16. Odish OFF, van den Berg-Huysmans AA, van den Bogaard SJA, et al. Longitudinal resting state fMRI analysis in healthy controls and premanifest Huntington's disease gene carriers: a three-year follow-up study. Hum Brain Mapp 2015;36(1):110–119. https://doi.org/10.1002/hbm.22616.
17. Smith SM, Fox PT, Miller KL, et al. Correspondence of the brain's functional architecture during activation and rest. Proc Natl Acad Sci U S A 2009;106(31):13040–13045. https://doi.org/10.1073/pnas.0905267106.
18. Vincent JL, Patel GH, Fox MD, et al. Intrinsic functional architecture in the anaesthetized monkey brain. Nature 2007;447:83–86. https://doi.org/10.1038/nature05758.
19. Allen EA, Damaraju E, Plis SM, Erhardt EB, Eichele T, Calhoun VD. Tracking whole-brain connectivity dynamics in the resting state. Cereb Cortex 2014;24(3):663–676. https://doi.org/10.1093/cercor/bhs352.
20. Power JD, Schlaggar BL, Lessov-Schlaggar CN, Petersen SE. Evidence for hubs in human functional brain networks. Neuron 2013;79(4):798–813. https://doi.org/10.1016/j.neuron.2013.07.035.
21. Yeo BTT, Krienen FM, Chee MWL, Buckner RL. Estimates of segregation and overlap of functional connectivity networks in the human cerebral cortex. Neuroimage 2014;88:212–227. https://doi.org/10.1016/j.neuroimage.2013.10.046.
22. Fiorenzato E, Strafella AP, Kim J, et al. Dynamic functional connectivity changes associated with dementia in Parkinson's disease. Brain 2019;142:2860–2872. https://doi.org/10.1093/brain/awz192.
23. Deco G, Jirsa VK, McIntosh AR. Emerging concepts for the dynamical organization of resting-state activity in the brain. Nat Rev Neurosci 2011;12(1):43–56. https://doi.org/10.1038/nrn2961.

24. Garrett DD, Kovacevic N, McIntosh AR, Grady CL. Blood oxygen level-dependent signal variability is more than just noise. J Neurosci 2010; 30(14):4914–4921. https://doi.org/10.1523/JNEUROSCI.5166-09.2010.

25. Dong D, Duan M, Wang Y, et al. Reconfiguration of dynamic functional connectivity in sensory and perceptual system in schizophrenia. Cereb Cortex 2019;29(8):3577–3589. https://doi.org/10.1093/cercor/bhy232.

26. Aracil-Bolaños I, Sampedro F, Marín-Lahoz J, et al. A divergent breakdown of neurocognitive networks in Parkinson's disease mild cognitive impairment. Hum Brain Mapp 2019;40(11):3233–3242. https://doi.org/10.1002/hbm.24593.

27. Penney JB, Vonsattel JP, MacDonald ME, Gusella JF, Myers RH. CAG repeat number governs the development rate of pathology in huntington's disease. Ann Neurol 1997;41(5):689–692. https://doi.org/10.1002/ana.410410521.

28. Nieto-Castanon A. Handbook of Functional Connectivity Magnetic Resonance Imaging Methods in CONN; Hilbert Press; 2020.

29. Desikan RS, Ségonne F, Fischl B, et al. An automated labeling system for subdividing the human cerebral cortex on MRI scans into gyral based regions of interest. Neuroimage 2006;31(3):968–980. https://doi.org/10.1016/j.neuroimage.2006.01.021.

30. Shirer WR, Ryali S, Rykhlevskaia E, Menon V, Greicius MD. Decoding subject-driven cognitive states with whole-brain connectivity patterns. Cereb Cortex 2012;22(1):158–165. https://doi.org/10.1093/cercor/bhr099.

31. Eickhoff SB, Yeo BTT, Genon S. Imaging-based parcellations of the human brain. Nat Rev Neurosci 2018;19(11):672–686. https://doi.org/10.1038/s41583-018-0071-7.

32. Sampedro F, Martínez-Horta S, Perez-Perez J, et al. Widespread increased diffusivity reveals early cortical degeneration in Huntington disease. Am J Neuroradiol 2019;40(9):1464–1468. https://doi.org/10.3174/ajnr.A6168.

33. Nanetti L, Contarino VE, Castaldo A, et al. Cortical thickness, stance control, and arithmetic skill: an exploratory study in premanifest Huntington disease. Parkinsonism Relat Disord 2018;51: 17–23. https://doi.org/10.1016/j.parkreldis.2018.02.033.

34. Paulsen JS, Miller AC, Hayes T, Shaw E. Cognitive and Behavioral Changes in Huntington Disease Before Diagnosis. 1st ed. Amsterdam, the Netherlands: Elsevier B.V.; 2017:144. https://doi.org/10.1016/B978-0-12-801893-4.00006-7

35. Dumas EM, Van Den Bogaard SJA, Hart EP, et al. Reduced functional brain connectivity prior to and after disease onset in Huntington's disease. Neuroimage Clin 2013;2(1):377–384. https://doi.org/10.1016/j.nicl.2013.03.001.

36. McColgan P, Razi A, Gregory S, et al. Structural and functional brain network correlates of depressive symptoms in premanifest Huntington's disease. Hum Brain Mapp 2017;38(6):2819–2829. https://doi.org/10.1002/hbm.23527.

37. Liu W, Yang J, Chen K, et al. Resting-state fMRI reveals potential neural correlates of impaired cognition in Huntington's disease. Parkinsonism Relat Disord 2016;27:41–46. https://doi.org/10.1016/j.parkreldis.2016.04.017.

38. Pini L, Jacquemot C, Cagnin A, et al. Aberrant brain network connectivity in presymptomatic and manifest Huntington's disease: a systematic review. Hum Brain Mapp 2020;41(1):256–269. https://doi.org/10.1002/hbm.24790.

39. Menon V, Uddin LQ. Saliency, switching, attention and control: a network model of insula function. Brain Struct Funct 2010;214: 655–667. https://doi.org/10.1007/s00429-010-0262-0.

40. Ciric R, Nomi JS, Uddin LQ, Satpute AB. Contextual connectivity: a framework for understanding the intrinsic dynamic architecture of large-scale functional brain networks. Sci Rep 2017;7(1):1–16. https://doi.org/10.1038/s41598-017-06866-w.

41. Ferreira LK, Regina ACB, Kovacevic N, et al. Aging effects on whole-brain functional connectivity in adults free of cognitive and psychiatric disorders. Cereb Cortex 2016;26(9):3851–3865. https://doi.org/10.1093/cercor/bhv190.

42. Peraza LR, Nesbitss D, Lawson R, et al. Intra- and inter-network functional alterations in Parkinson's disease with mild cognitive impairment. Hum Brain Mapp 2017;38(3):1702–1715. https://doi.org/10.1002/hbm.23499.

43. Seeley WW, Menon V, Schatzberg AF, et al. Dissociable intrinsic connectivity networks for salience processing and executive control. J Neurosci 2007;27(9):2349–2356. https://doi.org/10.1523/JNEUROSCI.5587-06.2007.

44. Goulden N, Khusnulina A, Davis NJ, et al. The salience network is responsible for switching between the default mode network and the central executive network: replication from DCM. Neuroimage 2014;99:180–190. https://doi.org/10.1016/j.neuroimage.2014.05.052.

45. Fox MD, Snyder AZ, Zacks JM, Raichle ME. Coherent spontaneous activity accounts for trial-to-trial variability in human evoked brain responses. Nat Neurosci 2006;9:23–25. https://doi.org/10.1038/nn1616.

46. Uddin LQ, Yeo BTT, Spreng RN. Towards a universal taxonomy of macro-scale functional human brain networks. Brain Topogr 2019;32(6):926–942. https://doi.org/10.1007/s10548-019-00744-6.

Supporting Data

Additional Supporting Information may be found in the online version of this article at the publisher's web-site.

SGML and CITI Use Only
DO NOT PRINT

Author Roles

1. Research Project: A. Conception, B. Organization, C. Execution; 2. Statistical Analysis: A. Design, B. Execution, C. Review and Critique; 3. Manuscript: A. Writing of the First Draft, B. Review and Critique.

I.A.-B.: 1A, 1B, 1C, 2A, 2B, 3A
S.M.-H.: 1A, 1B, 3B
J.M.G.-d.-E.: 2A, 2B, 2C, 3B
F.S.: 1C, 2A, 2B, 2C, 3B
J.P.-P.: 1A, 1B, 1C, 3B
A.H.-B: 1A, 1B, 1C, 3B
A.C.: 1B, 1C, 3B
C.I.: 1B, 1C, 3B
B.G.-A.: 1C, 3B
J.P.: 1A, 3B
J.K.: 1A, 1B, 1C, 3B

Financial Disclosures

Ignacio Aracil-Bolaños is supported by a research grant (CM19/00156 G) from the Instituto de Salud Carlos III (ISCIII). Frederic Sampedro is supported by a research grant from the government of Spain (ISCIII). Jose María González de-Echávarri is employed by Barcelonaβeta Brain Research Center and Pasqual Maragall Foundation and has received salary from Hospital de la Santa Creu I Sant Pau. Jaime Kulisevsky is employed by Hospital de la Santa Creu I Sant Pau and has received public research support from Centro de Investigación en Red-Enfermedades Neurodegenerativas (CIBERNED) and the Carlos III Institute, unrestrictive research support from Zambon and TEVA, and honoraria for lecturing and/or consulting from Zambon and TEVA. Javier Pagonabarraga is employed by Hospital de la Santa Creu I Sant Pau; has served on advisory or speakers' boards; received honoraria from UCB, Zambon, AbbVie, Italfarmaco, Allergan, Ipsen, and Bial; and received grants from CIBERNED and Fondo de Investigaciones Sanitarias (FIS) PI14/02058 (Spanish government grants) and Fundació La Marató de TV3 (20142910).